

The Information Of The Milky Way From 2MASS Whole Sky Star Count: The Bimodal Color Distributions

Chan-Kao Chang ¹

Institute of Astronomy, National Central University, Jhongli, Taiwan

Shao-Yu Lai

Institute of Astronomy, National Central University, Jhongli, Taiwan

Chung-Ming Ko ²

Institute of Astronomy, Department of Physics and Center of Complex Systems,
National Central University, Jhongli, Taiwan

and

Ting-Hung Peng

Institute of Astronomy, National Central University, Jhongli, Taiwan

Received _____; accepted _____

¹rex@astro.ncu.edu.tw

²cmko@astro.ncu.edu.tw

ABSTRACT

The $J - K_s$ color distribution (CD) with a bin size of 0.05 magnitude for the entire Milky Way has been carried out by using the Two Micron All Sky Survey Point Source Catalog (2MASS PSC). The CDs are bimodal, which has a red peak at $0.8 < J - K_s < 0.85$ and a blue peak at $0.3 < J - K_s < 0.4$. The colors of the red peak are more or less the same for the whole sky, but that of the blue peak depend on Galactic latitude ($J - K_s \sim 0.35$ at low Galactic latitudes and $0.35 < J - K_s < 0.4$ for other sky areas). The blue peak dominates the bimodal CDs at low Galactic latitudes and becomes comparable with the red peak in other sky regions. In order to explain the bimodal distribution and the global trend shown by the all sky 2MASS CDs, we assemble an empirical HR diagram, which is composed by observational-based near infrared HR diagrams and color magnitude diagrams, and incorporate a Milky Way model. In the empirical HR diagram, the main sequence stars turnoff of the thin disk is relatively bluer, $(J - K_s)_0 = 0.31$, when we compare with the thick disk which is $(J - K_s)_0 = 0.39$. The age of the thin/thick disk is roughly estimated to be around 4-5/8-9 Gyr according to the color-age relation of the main sequence turnoff. In general, the 2MASS CDs can be treated as a tool to census the age of stellar population of the Milky Way in a statistical manner and to our knowledge this is a first attempt to measure the age.

Subject headings: Galaxy: general - Galaxy: stellar content - Galaxy: structure
- stars: luminosity function, mass function - stars: Hertzsprung–Russell and C–M
diagrams - infrared: stars

1. Introduction

One of the obvious properties of the Milky Way that we want to learn is its morphology. The fact that we reside inside the Milky Way hinders us from a global view of our own Galaxy which we enjoy over other galaxies. William Herschel made use of star count (SC) to get a rough idea of how the Milky Way looks like in the eighteenth century (Herschel 1785). The advance in data collecting and analysis methods in late twentieth century let research groups (such as Bahcall & Soneira 1980; Gilmore & Wyse 1985) to quantify the major components (i.e., disks and halo) of our Galaxy by SC. They concluded that the properties of the stellar population in different components are distinguishable (see Table 1 in Chang et al. 2011, and references therein). Although many studies have been carried out, a common consensus on the structural parameters of the Milky Way has not been reached yet. One of the reasons can be attributed to different sky regions and limiting magnitudes (i.e., limiting volumes) were used (Siegel et al. 2002; Karaali et al. 2004; Bilir et al. 2006a,b; Karaali et al. 2007; Jurić et al. 2008). This problem can be overcome by wide sky coverage SC studies which become possible in the last decade as modern all sky surveys become available, such as the Two Micron All Sky Survey (2MASS; Skrutskie et al. 2006), the Sloan Digital Sky Survey (SDSS; York et al. 2000), the Panoramic Survey Telescope & Rapid Response System (Pan-Starrs; Kaiser et al. 2002) and the Wide-field Infrared Survey Explorer (WISE; Wright et al. 2010). However, subsequent researches did not settle the issue and the variation in different studies is thought to come from the degeneracy between the structural parameters. Moreover, the Galactic structural parameters have been reported to show dependence on Galactic longitude and latitude (Bilir et al. 2006a; Ak et al. 2007; Cabrera-Lavers et al. 2007; Bilir et al. 2008; Yaz et al. 2010). This makes the measurement and interpretation far more complex and challenging.

To solve the degeneracy, information other than SC is needed, e.g., dynamics, color, etc.

The most handy tool is stellar color as it is available in all sky surveys. That is the reason why most SC studies come with color distribution (CD), which calculates the number of star in each color bin. In addition to luminosity function (LF) and density profile (DP) used in single wavelength SC study, CD requires Hertzsprung-Russell diagram (HR diagram) to transform each luminous star into its corresponding color. HR diagram could be empirical (i.e., from observation) or theoretical (i.e., from population syntheses). In the empirical case, HR diagram and number densities of each spectral type star are provided from stellar cluster and local field stars (see e.g., Bahcall & Soneira 1980; Mamon & Soneira 1982; Wainscoat et al. 1992). Difficulties include time-consuming data collection and processing, and possible bias of sample selection (e.g., incompleteness, improper representation). In general, observational HR diagram in optical wavelength is obtained first and then other waveband HR diagrams are constructed by color transformation (see Mamon & Soneira 1982; Wainscoat et al. 1992, for examples). Thus, the uncertainty in color transformation needs to be considered carefully. In the theoretical case, HR diagram is deduced from the Hess diagram, which is generated by population synthesis based on knowledge of the initial mass function, stellar evolution and star formation history, etc. The Besançon model (Robin et al. 2003) and the TRILEGAL model (Girardi et al. 2005) are examples. Moreover, population synthesis models depend greatly on input parameters, and stellar evolution and atmosphere.

In Chang et al. (2010, 2011), we have shown that the K_s all sky 2MASS SCs can be well described by a single power law LF and a three-component DP (namely, the thin disk, the thick disk and the halo). In this work, we would like to extend our model to explain the $J - K_s$ CDs of the entire Milky Way. We gather currently available NIR data, i.e., from direct NIR observations, transformations of optical HR diagram, and observational NIR color magnitude diagram (CMD) of star clusters, to assemble an empirical NIR HR diagram and incorporate a Milky Way model to explain the 2MASS data. In a way, the HR

diagram we used is a 2MASS optimized HR diagram. The article is organized as follows. The features of the all sky 2MASS CD are described in section 2. Our Milky Way model, including LF and DP, is provided in section 3. The procedure to create our Hess diagram and HR diagram is given in section 4. In section 5 we present our results on CDs of the Milky Way, and section 6 is a summary and concluding remarks.

2. The 2MASS Data and Its Color Distributions

We use the 2MASS Point Source Catalog (2MASS PSC, Cutri et al. 2003) to carry out $J - K_s$ CDs with a bin size of 0.05 magnitude for the entire Milky Way. We select objects with the following criteria: (1) signal-to-noise ratio ≥ 5 , (2) detection in all J , H , K_s bands and (3) K_s magnitude between 5 and 14 mag. The last criterion ensures 99% completeness rate before the K_s limiting magnitude (i.e., 14.3 mag) and avoids the relatively large photometric error for $K_s \leq 5$ mag objects. The whole sky is divided into 8192 nodes according to level 5 Hierarchical Triangular Mesh (HTM, Kunszt et al. 2001), which samples the whole sky roughly evenly and has a 2 degrees angular separation on average. The radius of each node is 1 degree (i.e., each node covers π square degree). Because of the shallower limiting magnitudes and the complex extinctions in the Galactic center area, this work does not attempt to explain the 2MASS CDs in this region.

Several common features are identified in the whole sky 2MASS CDs, which are listed below and demonstrated in Fig. 1.

1. Most of the 2MASS CDs are bimodal, which has a blue peak at $0.3 < J - K_s < 0.4$ and a red peak at $0.8 < J - K_s < 0.85$. The 2MASS CDs at low Galactic latitudes have one more peak at $0.55 < J - K_s < 0.6$. Fig. 1a shows three examples of typical 2MASS CD at different Galactic latitudes.

2. The blue peak dominates the 2MASS CD at low Galactic latitudes and becomes comparable to the red peak at high Galactic latitudes. The middle peak only shows up at low Galactic latitudes and does not exist in other sky areas any more. Fig. 1b shows the averaged CDs over $225^\circ < l < 255^\circ$ at different Galactic latitudes.
3. The $J - K_s$ colors of the all sky red peaks and the middle peaks at low Galactic latitudes are almost fixed. However, the colors of the blue peak depend slightly on Galactic latitudes, which is $J - K_s \sim 0.35$ at low Galactic latitudes and $0.35 < J - K_s < 0.4$ at medium and high Galactic latitudes. The situation is demonstrated in Fig. 1c, which is the same as Fig. 1b except that the total count is normalized to $b = 10^\circ$. In contrast, the color of the blue peak does not change along Galactic longitude, see Fig. 1d & 1e.
4. We call the tapering off distribution on the blue side of the blue peak the blue wing. The shapes of the blue wings at different Galactic latitudes are very similar. Due to their bluer blue peaks, the blue wings of the CD at low Galactic latitudes can extend to $J - K_s = 0$. However, the blue wings at medium and high Galactic latitudes seldom extend to less than $J - K_s = 0.2$. The normalized 2MASS CDs in Fig. 1c clearly shows this property.
5. Occasionally, some 2MASS CDs at medium or high Galactic latitudes have a middle peak, which is different from the middle peak at low Galactic latitudes. We call it ‘the extra peak’ and will explain more in section 4.1 and 4.2. The solid lines in the first column of Fig. 2 show three examples of the extra peak.
6. The shape of the 2MASS CD can be altered significantly by severe extinction, which is the usual case at low Galactic latitudes. Fig. 3 shows the 2MASS CDs at $|b| \sim 16^\circ$. The figures are arranged according to their $E(J - K_s)$ extinction values. As the $E(J - K_s)$ values increase, the sharpness of the 2MASS CDs decrease gradually, and

the $J - K_s$ colors of the blue and middle peaks become redder and redder. Moreover, the tail in the red end is elongated.

3. The Milky Way Model

Our Milky Way model has a three-component DP and a single power law LF (Chang et al. 2010, 2011). The three-component DP $n(R, Z)$ includes a thin disk D_1 , a thick disk D_2 and an oblate halo S ,

$$n(R, Z) = n_0 [D_1(R, Z) + D_2(R, Z) + S(R, Z)] , \quad (1)$$

where R is the galactocentric distance on the Galactic plane, Z is the distance from the Galactic mid-plane and n_0 is the local stellar density of the thin disk at the solar neighborhood.

The disks are in a double exponential decay form in which stellar density decreases exponentially along R and Z ,

$$D_i(R, Z) = f_i \exp \left[- \frac{(R - R_\odot)}{H_{ri}} - \frac{(|Z| - |Z_\odot|)}{H_{zi}} \right] , \quad (2)$$

where (R_\odot, Z_\odot) is the location of the Sun, H_{ri} is the scale-length, H_{zi} is the scale-height, and f_i is the density ratio to the thin disk at the solar neighborhood. The subscript $i = 1$ stands for the thin disk and $i = 2$ stands for the thick disk.

The halo is a power law decay oblate spheroid flattening in the Z direction,

$$S(R, Z) = f_h \left[\frac{R^2 + (Z/\kappa)^2}{R_\odot^2 + (Z_\odot/\kappa)^2} \right]^{-p/2} , \quad (3)$$

where κ is the axis ratio, p is the power index and f_h is the local halo-to-thin disk density ratio.

The M_{K_s} LF is a single power law (Chang et al. 2010),

$$\psi(M_{K_s}) = \frac{2 \log_e 10 (\gamma - 1)}{5 [10^{2(\gamma-1)M_f/5} - 10^{2(\gamma-1)M_b/5}]} 10^{2(\gamma-1)M/5}, \quad (4)$$

where γ is the power law index, M_b and M_f are the bright and faint cutoffs, respectively. Note that $\psi(M)$ includes all luminosity classes. For convenience, we adopt the peak values of the bright end and faint end distributions of Chang et al. (2010), i.e., $M_b = -8$ and $M_f = 6.5$ (see Fig. 6 in Chang et al. 2010), as the bright and faint ends in this study. We note that the averages in Chang et al. (2010) are $M_b = -7.86 \pm 0.60$ and $M_f = 6.88 \pm 0.66$. Nevertheless, the model prediction shows no significant difference between using the peak values and the average ones.

The extinction model is adopted from the new COBE/IRAS result (Chen et al. 1999) and the color excess is $E(J - K_s)/E(B - V) = 0.53$ (Schlegel et al. 1998). Table 1 lists the parameters taken from Chang et al. (2010) and Chang et al. (2011) (hereafter MW-I).

4. The Empirical NIR HR Diagram Optimized for the 2MASS CD

We describe the search for an empirical NIR HR diagram (tailored for 2MASS data) in three subsections for a simple and clear exposition.

4.1. Basic NIR HR Diagram

We take observational-based NIR HR diagrams in the literature as our first construction of the loci of main sequence (MS) and giant branch (GB) in $M_{K_s}-(J - K_s)_0$ HR diagram. Wainscoat et al. (1992, hereafter W92) and Covey et al. (2007, hereafter C07) have the information of NIR HR diagram (i.e., the NIR color, absolute magnitude and spectral type). W92 also gives the number density in the solar neighborhood and the normalization

in different components of Milky Way. Fig. 4 shows the data points of MS, GB and super giants taken from W92 and C07. Both data sets agree to each other very well and shows several common features: (1) a sharp downturn around the end of MS (hereafter, MS-downturn), (2) a slight upturn around late A type star (i.e., $M_{K_s} \sim 3$ mag and hereafter, MS-turnoff), and (3) a sharp curve on GB around $M_{K_s} \sim -1$ mag (hereafter, GB-curve). We fit W92 data to find the loci and integrate it with MW-I to obtain a synthetic CD. When the synthetic CD is compared with 2MASS CD, some significant discrepancy is observed: (1) over predictions for the middle peak and for the blue wing (i.e., $J - K_s < 0.3$ mag), (2) under prediction on the blue peak, and (3) the locations of the blue and middle peaks are not correct. The first column in Fig. 5 demonstrates several results for different Galactic latitudes. However, we obtain a very useful information that the $J - K_s$ colors of each peak correspond to that of each sharp turn (or ‘vertical’ sections) on the loci. Apparently, the blue, red and middle peaks are the results of the MS-turnoff around late A type stars, the MS-downturn and the GB-curve, respectively.

4.2. The Optimization for the Empirical NIR HR Diagram

To study the sharp turns in more detail, we utilize several NIR CMDs of star clusters from the literature, such as Beletsky et al. (2009); Sarajedini et al. (2009); Troisi et al. (2010). Some of them (e.g., M67 and NGC6791 in Beletsky et al. 2009; Sarajedini et al. 2009), which have information down to the faint end of MS, are used to conclude the important features for our analysis: (1) the MS-downturn $(J - K_s)_0 \sim 0.83$ is a common feature at the faint end of MS; (2) the MS-turnoff (i.e., the slight upturn around late A star) reflects stars departing from the MS at the end of their MS stage; (3) the MS-turnoff always accompanies a $\Delta M_{K_s} \sim 2.5 K_s$ mag vertical height extension and its $(J - K_s)_0$ color depends on the age of the star cluster; and (4) the main sequence belt between the

MS-turnoff and the MS-downturn is approximately linear. Since only few GB stars are shown on these NIR CMDs, we are not able to get more details of the GB-curve. However, we believe that the location of the GB-curve should be similar to that of W92 and C07.

Accordingly, a working HR diagram includes the following features. The MS is divided into three parts: (1) early MS (i.e., O-A type stars and $M_{K_s} \lesssim 3$ mag); (2) nearly linear late MS (i.e., F-K type stars and $3 \lesssim M_{K_s} \lesssim 5$ mag); and (3) sharp and almost vertical MS-downturn at $(J - K_s)_0 \sim 0.83$ (i.e., M type and later stars and $M_{K_s} \gtrsim 5$ mag). The GB is separated into up and low GBs. Both are linear and connected by the GB-curve at $(J - K_s)_0 \sim 0.6$ and $M_{K_s} \sim -1$. Consequently, we create an empirical M_{K_s} against $(J - K_s)_0$ locus including a vertical MS-downturn, a linear late MS, a MS-turnoff with a $\Delta M_{K_s} = 2.5 K_s$ mag vertical extension, a linear low GB, a linear up GB and a flat transition between the tip of the MS-turnoff and the low GB. The slopes of each linear part (i.e., the up GB, the low GB and the late MS) and the connecting joints of different parts are taken from the CMDs mentioned above and the data in W92 and C07. The early MS is not included because the 2MASS CDs are generally deficient in number of stars in the region $(J - K_s)_0 < 0.2$. Since the $J - K_s$ colors of the red peak of 2MASS CD is between 0.8 to 0.85 and that of the MS-downturns of M67 and NGC6791 are at ~ 0.83 (Beletsky et al. 2009; Sarajedini et al. 2009), we set $(J - K_s)_0 = 0.83$ for the vertical MS-downturn. Moreover, the middle peak is around $J - K_s = 0.55$ to 0.6 and the GB-curves in W92 and C07 also have similar color, so we set $(J - K_s)_0 = 0.6$ for the GB-curve and let the low GB between $(J - K_s)_0 = 0.5$ and 0.6. To incorporate the idea that different $(J - K_s)_0$ colors of the MS-turnoff for different evolutionary stage populations (Sarajedini et al. 2009), we allow the MS-turnoff to move along the main sequence belt. The left panel of Fig. 4 shows the empirical NIR locus on top of the data points taken from W92, C07 and M67 (Beletsky et al. 2009). To mimic observational color scattering, we put a 0.06 color dispersion to the empirical locus (see the right panel of Fig. 4).

Incorporating this empirical NIR HR diagram with MW-I, we found several features in the model prediction (see Fig. 5): (1) the CD generated by the thin disk is a bimodal distribution; (2) the CD generated by the thick disk only shows the blue peak; (3) both CDs of the thin and thick disk can have a middle peak at low Galactic latitudes; (4) the overall model prediction is mainly dominated by the CD of the thin disk; (5) the blue peak of the thick disk has an appreciable contribution to that of the overall model prediction only at medium and high Galactic latitudes; and (6) the red peak of the overall model prediction is determined mostly by the thin disk.

At first, we focus on medium and high Galactic latitudes to avoid severe extinction. The $(J - K_s)_0$ colors of the MS-turnoff for the thin and thick disk are set between 0.35 and 0.4 to comply with the blue peak of 2MASS CD at medium and high latitudes. We integrate the empirical locus (Fig. 4) with our Milky Way model MW-I to generate the synthetic CD. For reasonable good fit, the $(J - K_s)_0$ color of the thin disk and the thick disk are found to be 0.34-0.35 and 0.38-0.39, respectively. The second column in Fig. 5 shows some results at different Galactic latitudes.

The result at medium and high Galactic latitudes agrees well with the 2MASS data. Then, we inspect low Galactic latitudes which have relatively small extinction. The result shows significant difference in the blue wing of the blue peak (i.e., $J - K_s < 0.3$), but the rest of the CD is still in a good agreement (see the first row of the second column in Fig. 5). If a bluer turnoff is assigned to the thin disk, the discrepancy in the blue wing can be compensated somewhat, but it will cause an over prediction in the blue wing and a shift in $J - K_s$ color of the blue peak at high Galactic latitudes (see the third column in Fig. 5).

4.3. The Final Adjustment

When experimenting parameters of the model in previous subsections, we notice a small scale height thin disk would make its blue peak change more dramatically along Galactic latitude. This makes the overall blue peak (i.e., the thin and thick disks) at low Galactic latitudes be dominated by the thin disk, while the blue peak at medium and high Galactic latitudes be dominated by the thick disk. Therefore, a small scale height thin disk with a bluer MS-turnoff not only can eliminate the difference in the blue wing at low Galactic latitudes, but also can reduce its contribution to the blue peak at medium and high Galactic latitudes. In this way, the $J - K_s$ color of the blue peak could be relatively bluer at low Galactic latitudes and relatively redder at the other sky region. With this strategy, we select an acceptable Galactic structure configuration with a relatively smaller scale height thin disk from our previous SC study (see Chang et al. 2011, for details) and come up with the best fit model as follows: (1) the scale height of the thin disk is $H_{z1} = 260$ pc and other structural parameters are listed in Table 1 (hereafter, MW-II); and (2) the MS-turnoff of the thin disk is $(J - K_s)_0 = 0.31$ mag. With this model, the 2MASS CDs at low Galactic latitudes can be fitted much better than that in subsection 4.2 (see the last column in Fig. 5).

Fig. 4 shows the HR diagram obtained from subsections 4.2 and 4.3. Incorporating the luminosity function derived from 2MASS SC (Chang et al. 2010), we construct the Hess diagram of MW-II in the right panel of Fig. 4. The joints on the HR diagram of MW-II are listed in Table 2.

5. Results and Discussion

In Figs. 6 & 7 we compare our model prediction (i.e., MW-II in section 4.3) and the 2MASS CDs at different Galactic latitudes. In order to minimize the uncertainty caused by extinction correction at low Galactic latitudes, we compare sky areas with relatively small extinction. The model prediction and the 2MASS CD agree very well in the overall shape and the $J - K_s$ color of each peak. The number variations along Galactic latitudes of each peak are well reproduced by the model.

In order to present the global trend of the 2MASS CDs, we show the number ratio of the blue part (i.e., $J - K_s \leq 0.6$) to the red part (i.e., $J - K_s > 0.6$) in Fig. 8 along with the prediction of MW-II. Both figures have very similar trend which is relatively blue at low Galactic latitudes and become comparable in other sky regions. The very red Galactic disk is the result of severe extinction.

When we inspect the Galactic disk region (i.e., $|b| < 10^\circ$), the model prediction has obvious discrepancy with the 2MASS CD. The discrepancy can mostly be attributed to improper extinction correction and number inconsistency between the model prediction and the 2MASS data. The number inconsistency, which has been reported in Chang et al. (2011), results in gaps on each peak between the model prediction and the 2MASS CD. Fig. 9 demonstrates some cases together with the SC results taken from Chang et al. (2011). In these cases, the sky areas have relatively small extinction. This helps us to delineate the discrepancy mainly comes from the number inconsistency (see the difference in SC result, lower panels in Fig. 9). Several examples of improper extinction correction are illustrated in the first column of Fig. 10. The improper extinction can make a significant offset on the $J - K_s$ colors of the blue and middle peaks and distort the shape of CD. Moreover, we also find a significant blue population (i.e., $J - K_s < 0.2$) in the 2MASS CD on the Galactic disk ($|b| < 10^\circ$) around the Galactic longitudes of $180^\circ < l < 240^\circ$ (see the second column

of Fig. 10). This blue population is neither predicted by the model nor the blue wing of the blue peak. If we omitted the extinction correction, the model still cannot account for such a blue population. The origin of this blue population warrants further studies.

Several 2MASS CDs at medium and high Galactic latitudes have an extra peak at $J - K_s \sim 0.55$. Their occurrence and height do not correlate with Galactic coordinates. Most of them are insignificant, but we show three good examples in the first column of Fig. 2 (solid line). We note that each example has a globular cluster within the field of view. In order to nail down the origin of the extra peak, we generate globular-cluster-only CD (dashed line). Each globular-cluster-only CD has a spike, which has $J - K_s$ color very similar to that of the extra peak in the whole field CD (i.e., the CD contains stars both from the globular cluster and the field; solid line). We also obtain the CD of the ambient field (dot-dashed line) by subtracting the globular-cluster-only CD from the whole field CD. The extra peak does not show up anymore in the ambient field CD. Besides, each globular cluster CMD has an obvious GB with an obscure GB-curve at $J - K_s \sim 0.55$ similar to that on the empirical HR diagram (see Fig. 4). Therefore, we conclude that the extra peak is due to the low GB of the globular cluster and its significance depends on the relative amount of star in the low GB of the globular cluster to that in the ambient field. Besides, if the limiting magnitude could be reached down to the MS-turnoff of the globular clusters, the observed blue peak would have more stars than the model prediction. Similar number enhancement could happen in the 2MASS CDs if there is an overdensity within the field of view, which have a dominant stellar population over the smooth stellar distribution of the Milky Way (e.g., star cluster, stellar stream, Galactic bulge, Galactic arm, etc.). For instance, the extremely dense Galactic bulge, which is not included in our model, makes a prominent middle peak on the 2MASS CDs, which obviously outnumbers the model prediction (see the third column of Fig. 10). However, we do not observe any obvious number enhancement in other 2MASS CDs which have known stellar streams in

their field of view, e.g., Sagittarius dwarf galaxy (Majewski et al. 2003), Monoceros stream (Peñarrubia et al. 2005, ; Table 1), etc. It is possible that within the 2MASS detection limit the populations of these overdensities are too small.

At low Galactic latitudes there is another possible way to generate the middle peak. It is the red clump stars (Alves 2000; Cabrera-Lavers et al. 2007), which occupies the space close to the low GB on our HR diagram and has a higher number density relative to the other stars on GB. Such relatively higher number density would produce more stars in the corresponding color bins. In our model we do not include the red clump stars in our LF and HR diagram, but our model still has good agreement with the 2MASS CD. The reason might be the net contribution of the red clump stars in generating the middle peak is similar to that of the low GB.

Our best model that can explain the all sky 2MASS CDs (see section 4.3) comprises a thin disk, which has a relative short scale height (260 pc) and a relative blue MS-turnoff (i.e., younger), and a thick disk (1040 pc), which has a relative red MS-turnoff (i.e., older). Our best model, MW-II, that can explain the all sky 2MASS CDs (see section 4.3) comprises a thin disk (260 pc) with a relatively blue MS-turnoff (0.31 mag, i.e., younger), and a thick disk (1040 pc) with a relatively red MS-turnoff (0.38 mag, i.e., older). The two populations can be interpreted in the context of the formation of the Milky Way. The thick disk was formed in an epoch earlier than the thin disk. Moreover, both disks have the same single power law LF which implies that the initial mass function does not change along the Milky Way’s evolution (unless the mass-luminosity relation was time dependent in the past). In this sense, the all sky 2MASS CDs can be used as a tool to census the age of stellar population in the Milky Way. If we apply the color-age relation of MS-turnoff of Sarajedini et al. (2009) to our empirical HR diagrams, we can roughly estimate the ages of the thin and thick disk to be 4-5 Gyr and 8-9 Gyr, respectively. The age estimation

should be viewed as the lower limit. The blue boundary of the 2MASS CDs do not allow bluer MS-turnoffs of the disks. Moreover, the 0.05 mag bin size of our 2MASS CD can only provide a low color resolution of the blue peak, hence the color of the MS-turnoff and the derived age cannot be estimated more precisely. Nevertheless, to the best of our knowledge our result could be the first attempt to measure the age of global stellar components in a general statistical sense. We conclude that the whole population of the thick disk is about 3-4 Gyr older than that of the thin disk.

In this work, we seldom mention the halo component because it has very limited contribution to the total CDs in magnitude range we are interested (i.e., $4 \text{ mag} < K_s < 14 \text{ mag}$). Thus, we are not able to extract solid and useful information of the halo from 2MASS CD.

6. Summary

We use 2MASS PSC to carry out the whole sky $J - K_s$ CDs, which show a bimodal distribution with a blue peak and a red peak. The blue peak is the dominant feature at low Galactic latitudes and becomes comparable to the red peak at high Galactic latitudes. The all sky $J - K_s$ colors of the red peak are almost the same (between 0.8 and 0.85 mag). However, the $J - K_s$ colors of the blue peak at low Galactic latitudes are a bit bluer (0.35 mag) than that at medium and high Galactic latitudes (between 0.35 mag and 0.4 mag). However, the $J - K_s$ colors of the blue peak at low Galactic latitudes are a bit bluer (which is $J - K_s \sim 0.35$) than that at medium and high Galactic latitudes (which is between 0.35 and 0.4). Besides, a middle peak shows up at $J - K_s \sim 0.55$ at low Galactic latitudes and does not exist in other sky areas. Several medium and high Galactic latitudes have an extra peak at $J - K_s \sim 0.55$, which is not the same as the middle peak at low Galactic latitudes.

In order to explain the whole sky 2MASS CDs, we create an empirical M_{K_s} against $J - K_s$ HR diagram optimized for the 2MASS data by gathering available NIR HR diagrams and CMDs (Wainscoat et al. 1992; Covey et al. 2007; Beletsky et al. 2009; Sarajedini et al. 2009; Troisi et al. 2010) and incorporate a Milky Way model (Chang et al. 2010, 2011). The HR diagram of the thin disk has a bluer MS-turnoff (i.e., younger), and that of the thick disk has a redder MS-turnoff (i.e., older). For a better explanation of the 2MASS CDs, the result is in favor of a relatively small scale height thin disk (260 pc, MW-II, compare with 360 pc in MW-I; other parameters of MW-I and MW-II are given in Table 1). We note that the configuration of MW-II is within the ‘acceptable’ solutions due to the degeneracy between the structural parameters, which has been pointed out as a problem for using SC to study the Galactic structure (e.g., Chang et al. 2011). Now information from CD helps to rule out the degeneracy, and we deem that MW-II should be the preferred model.

We find that the blue peak, the red peak and the middle peak are due to the MS-turnoff, the MS-downturn and the GB-curve, respectively (see Fig. 4). Moreover, the extra peak at some medium or high Galactic latitudes is due to globular clusters. Our model cannot trace the CDs which suffer severe extinction and need a more elaborate extinction correction.

When we apply the color-age relation of the MS-turnoff (Sarajedini et al. 2009) to our empirical HR diagram, the thin and thick disks are estimated to be around 4-5 Gyr and 8-9 Gyr, respectively. The idea is consistent with the Milky Way’s formation theory. We realize that the whole sky 2MASS CDs can be used as a tool to census the age of stellar populations of the Milky Way in a statistical manner. To the best of our knowledge, this study is the first attempt to measure the ages of the thin and thick disks from the whole sky stellar population.

It is no doubt that the 2MASS PSC provides an unique tool to study the global property of the Milky Way, not only for its tremendous sky coverage (which avoids the

selection effect of limited sky coverage), but also for the benefits of using NIR wavelength (which keeps fine angular resolution and is less affected by interstellar extinction).

We acknowledge the use of the Two Micron All Sky Survey Point Source Catalog (2MASS PSC). This work is supported in part by the National Science Council of Taiwan under the grants NSC-98-2923-M-008-001-MY3 and NSC-99-2112-M-008-015-MY3.

Table 1. The Milky Way model.

	MW-I	MW-II
Density Profile		
Thin Disk		
H_{r1}	3.7 kpc	3.7 kpc
H_{z1}	360 pc	260 pc
n_0	0.030 stars/pc ³	0.039 stars/pc ³
Z_{\odot}	25 pc	
R_{\odot}	8 kpc (Reid 1993)	
Thick Disk		
H_{r2}	5.0 kpc	5.0 kpc
H_{z2}	1020 pc	1040 pc
f_2	7%	10 %
Spheroid		
κ	0.55	
p	2.6	
f_h	0.20%	
M_{K_s} Luminosity Function		
γ	1.85	
M_b	-8	
M_f	6.5	
Extinction Correction		
new COBE/IRAS result (Chen et al. 1999)		
$E(J - K_s)/E(B - V)$	0.53 (Schlegel et al. 1998)	

Table 2. The Empirical HR Diagram Optimized for 2MASS.

Part	$(J - K_s)_0$	M_{K_s}
Common Joints		
Faint End of MS	0.83	6.5
MS-Downturn	0.83	5.0
GB-Curve	0.6	-1.0
Bright End of Up GB	1.4	-8.0
Thin Disk		
MS-Turnoff	0.31	3.34
Bright End of MS-Turnoff	0.31	0.84
Faint End of Low GB	0.54	0.34
Thick Disk		
MS-Turnoff	0.38	3.56
Bright End of MS-Turnoff	0.38	1.06
Faint End of Low GB	0.53	0.56

REFERENCES

- Ak, S., Bilir, S., Karaali, S., & Buser, R. 2007, *Astronomische Nachrichten*, 328, 169
- Alves, D.R. 2000, *ApJ*, 539, 732
- Bahcall, J.N., & Soneira, R.M. 1980, *ApJ*, 238, 17
- Beletsky, Y., Carraro, G., & Ivanov, V. D. 2009, *A&A*, 508, 1279
- Bilir, S., Karaali, S., Ak, S., Yaz, E., & Hamzaoglu, E. 2006a, *New A*, 12, 234
- Bilir, S., Karaali, S., & Gilmore, G. 2006b, *MNRAS*, 366, 1295
- Bilir, S., Cabrera-Lavers, A., Karaali, S., Ak, S., Yaz, E., & López-Corredoira, M. 2008, *PASA*, 25, 69
- Cabrera-Lavers, A., Bilir, S., Ak, S., Yaz, E., & López-Corredoira, M. 2007, *A&A*, 464, 565
- Chang, C.-K., Ko, C.-M., & Peng, T.-H. 2010, *ApJ*, 724, 182
- Chang, C.-K., Ko, C.-M., & Peng, T.-H. 2011, *ApJ*, 740, 34.
- Chen, B., Figueras, F., Torra, J., Jordi, C., Luri, X., & Galadi-Enriquez, D. 1999, *A&A*, 352, 459
- Covey, K. R., Ivezić, Ž., Schlegel, D., et al. 2007, *AJ*, 134, 2398
- Cutri, R.M., et al. 2003, The IRSA 2MASS All-Sky Point Source Catalog, NASA/IPAC Infrared Science Archive. <http://irsa.ipac.caltech.edu/applications/Gator/>
- Gilmore, G., & Wyse, R. F. G. 1985, *AJ*, 90, 2015
- Girardi, L., Groenewegen, M.A.T., Hatziminaoglou, E., & da Costa, L. 2005, *A&A*, 436, 895

- Herschel, W. 1785, Royal Society of London Philosophical Transactions Series I, 75, 213
- Jurić, M., et al. 2008, ApJ, 673, 864
- Kaiser, N., et al. 2002, Proc. SPIE, 4836, 154
- Karaali, S., Bilir, S., & Hamzaoğlu, E. 2004, MNRAS, 355, 307
- Karaali, S., Bilir, S., Yaz, E., Hamzaoğlu, E., & Buser, R. 2007, PASA, 24, 208
- Kunszt, P.Z., Szalay A.S., & Thakar A.R. 2001, Proc. of the MPA/ESO/MPE workshop (Springer-Verlag Berlin Heidelberg), pp. 631
- Majewski, S. R., Skrutskie, M. F., Weinberg, M. D., & Ostheimer, J. C. 2003, ApJ, 599, 1082
- Mamon, G. A., & Soneira, R. M. 1982, ApJ, 255, 181
- Peñarrubia, J., Martínez-Delgado, D., Rix, H. W., et al. 2005, ApJ, 626, 128
- Reid, M. J. 1993, ARA&A, 31, 345
- Robin, A. C., Reylé, C., Derrière, S., & Picaud, S. 2003, A&A, 409, 523
- Sarajedini, A., Dotter, A., & Kirkpatrick, A. 2009, ApJ, 698, 1872
- Schlegel, D.J., Finkbeiner, D.P., & Davis, M. 1998, ApJ, 500, 525
- Siegel, M. H., Majewski, S. R., Reid, I. N., & Thompson, I. B. 2002, ApJ, 578, 151
- Skrutskie, M.F., et al. 2006, AJ, 131, 1163
- Troisi, L., Bono, G., Dall’Ora, M., et al. 2010, Memorie della Societa Astronomica Italiana Supplementi, 14, 139
- Yaz, E., Bilir, S., Karaali, S., et al. 2010, Astronomische Nachrichten, 331, 807

York, D. G., et al. 2000, AJ, 120, 1579

Wainscoat, R. J., Cohen, M., Volk, K., Walker, H. J., & Schwartz, D. E. 1992, ApJS, 83,
111

Wright, E. L., Eisenhardt, P. R. M., Mainzer, A. K., et al. 2010, AJ, 140, 1868

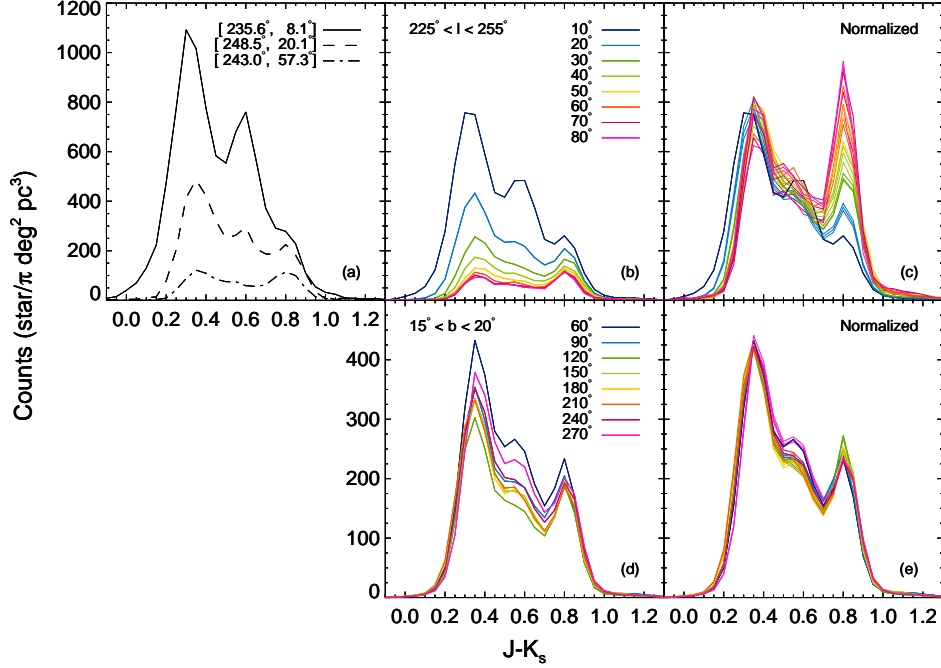


Fig. 1.— Salient features on the 2MASS CD. (a) Typical examples of 2MASS CD, $[l, b] = [235.6^\circ, 8.1^\circ]$ (solid line), $[248.5^\circ, 20.1^\circ]$ (dashed line) and $[243.0^\circ, 57.3^\circ]$ (dotted-dashed line). (b) The 2MASS CDs averaged over $225^\circ < l < 255^\circ$ at different Galactic latitudes. The Galactic latitudes are indicated by different colors. (c) Same as (b), except that the total count is normalized to that of $b = 10^\circ$. (d) The 2MASS CDs averaged over $15^\circ < b < 20^\circ$ at different Galactic longitudes. The Galactic latitudes are indicated by different colors. (e) Same as (d), except that the total count is normalized to that of $l = 60^\circ$.

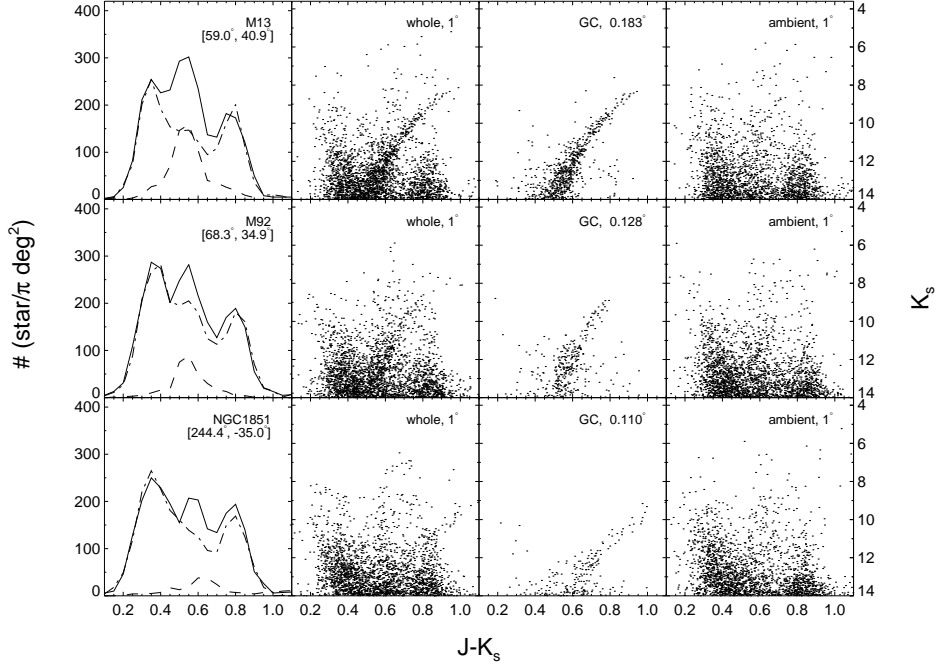


Fig. 2.— The first column is the 2MASS CMDs having the extra peak at medium and high Galactic latitudes. The whole field, the globular-cluster-only and the ambient field CMDs are represented by the solid, dashed and dotted-dashed lines, respectively. The identification of the star cluster and its center coordinate are indicated on the upper-right corner of each figure. The second, third and last columns show the CMDs of the whole field, the globular-cluster-only and the ambient field, respectively. The radii of the field of view of the whole field and the ambient field CMDs are 1 degree and that of globular-cluster-only CMD is given on the upper-right corner of each figure in the third column.

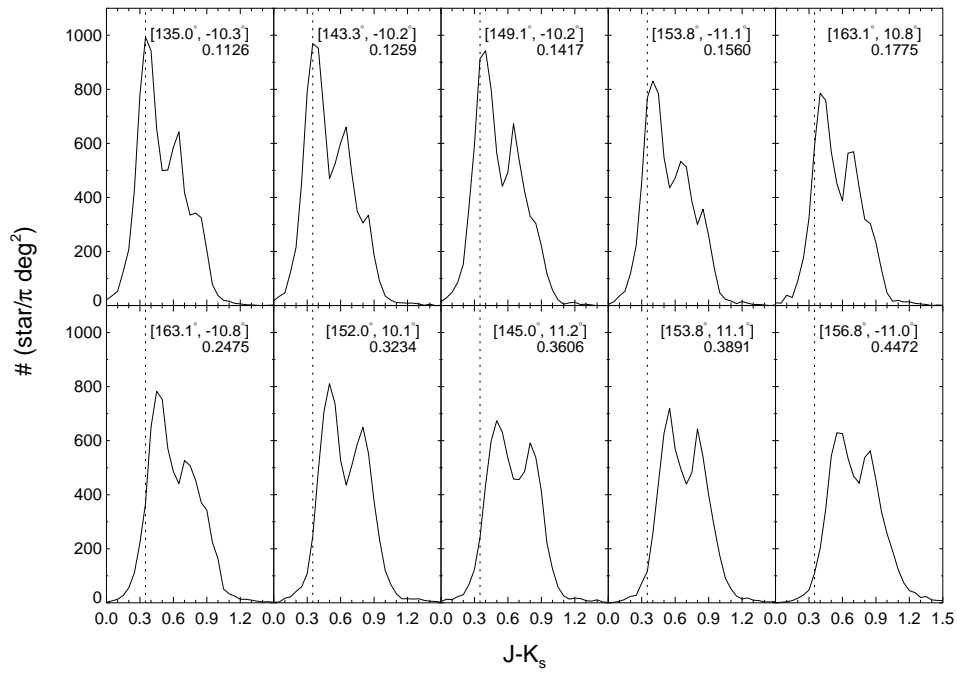


Fig. 3.— The 2MASS CDs around $|b| \sim 16^\circ$ with different $E(J - K_s)$ extinction values. The legend gives the Galactic coordinates and the $E(J - K_s)$ value.

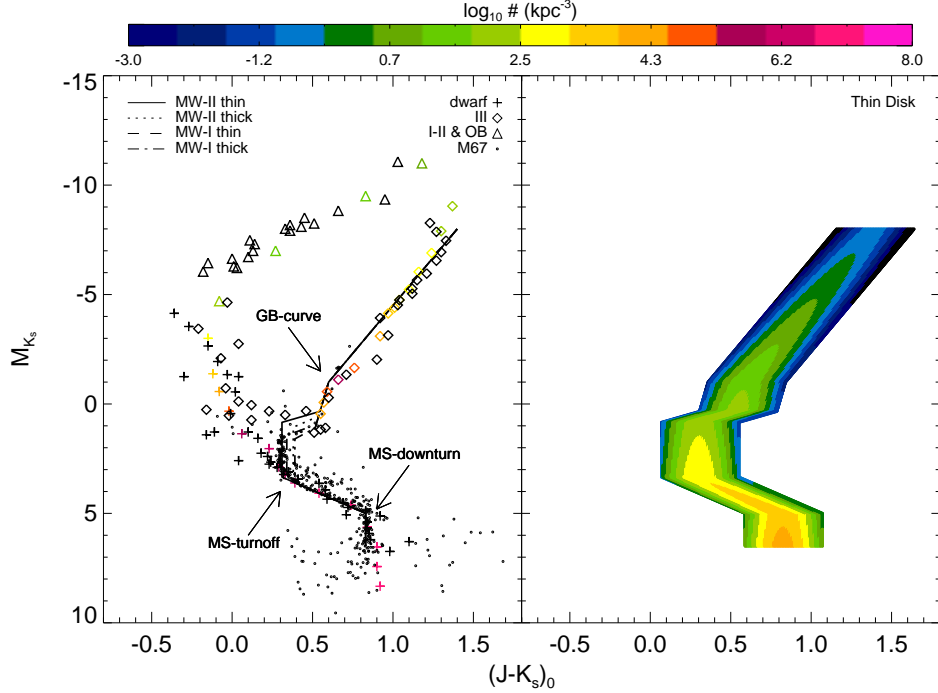


Fig. 4.— The HR diagram and the Hess diagram. The left panel is the NIR HR diagram. The data points are taken from W92 (color symbols), C07 (black symbols) and M67 (small black open circle; Beletsky et al. 2009). The upper-right legend indicates luminosity classes and the number density is coded by the color bar. C07 does not have number density information, so it is plotted as black. Each small black open circle represents one member star of M67. The lines represent different HR diagrams used in subsections 4.2, 4.3. The upper-left legend gives the corresponding models and components. The right panel is the Hess diagram of the thin disk used in MW-II whose number density is color coded.

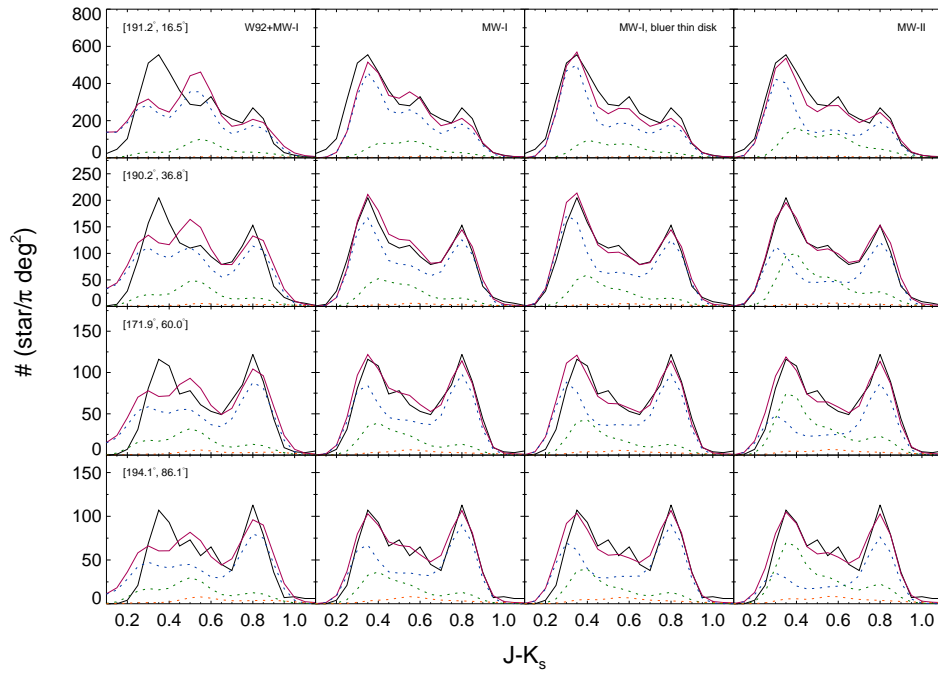


Fig. 5.— The synthetic CDs of different HR diagrams (see section 4 for details). Black line is the 2MASS data, and pink line is the model prediction. The blue, green and orange dotted lines represent the thin disk, the thick disk and the halo, respectively.

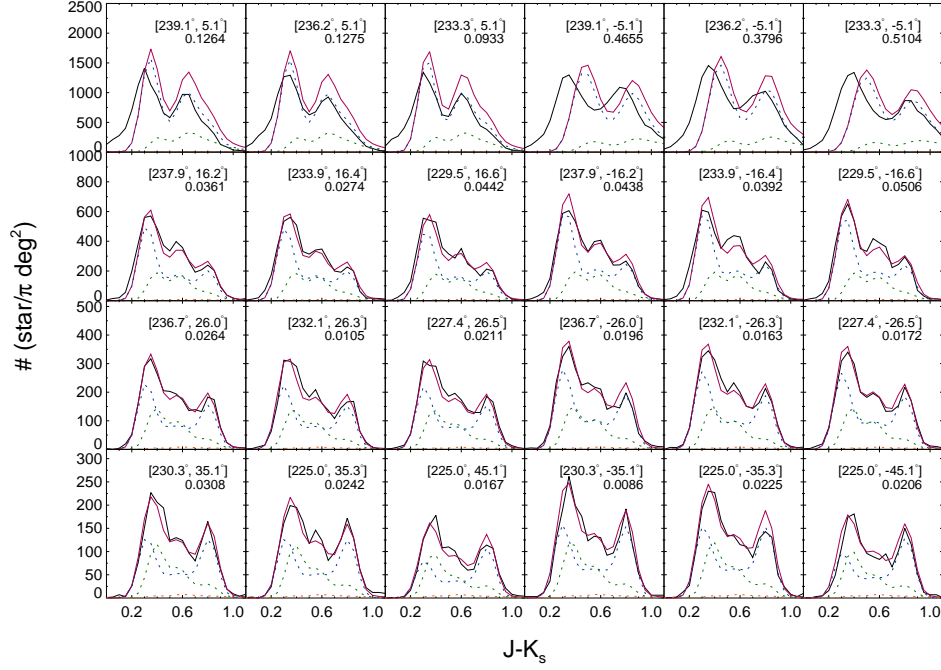


Fig. 6.— Comparison between 2MASS CDs (black) and model predictions (pink). The coordinates and the extinction $E(J - K_s)$ are given at the upper-right corner of each figure. The blue, green and orange dotted lines represent the thin disk, the thick disk and the halo, respectively.

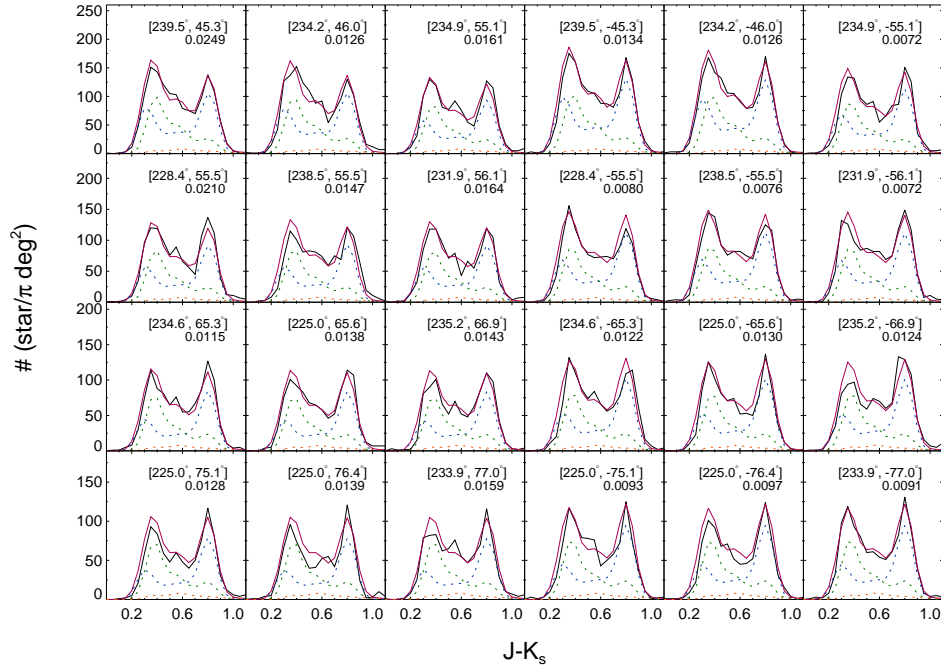


Fig. 7.— Continuation of Fig. 6.

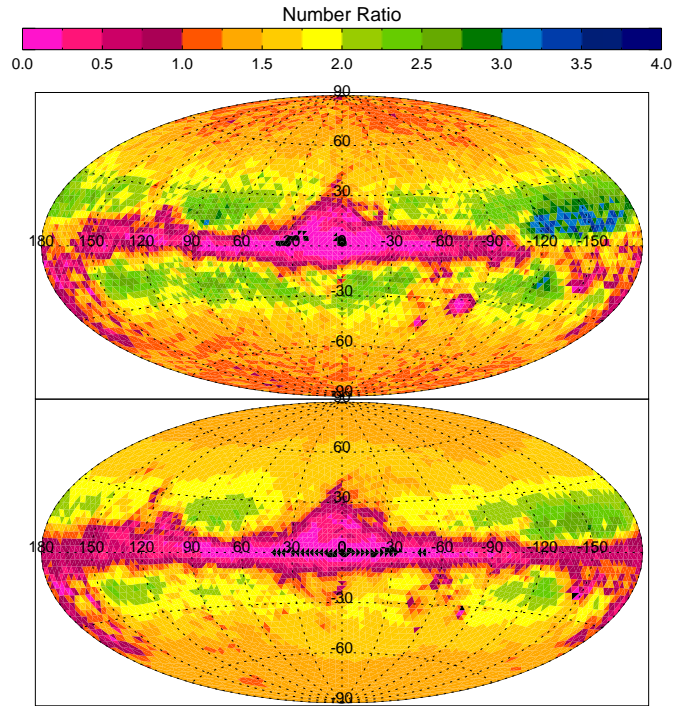


Fig. 8.— The number ratio of the blue part ($J - K_s < 0.6$) to the red part ($J - K_s > 0.6$). Top: 2MASS data. Bottom: model prediction. Note that the very red Galactic disk is the result of severe extinction and it does not reflect the intrinsic number ratio in these regions.

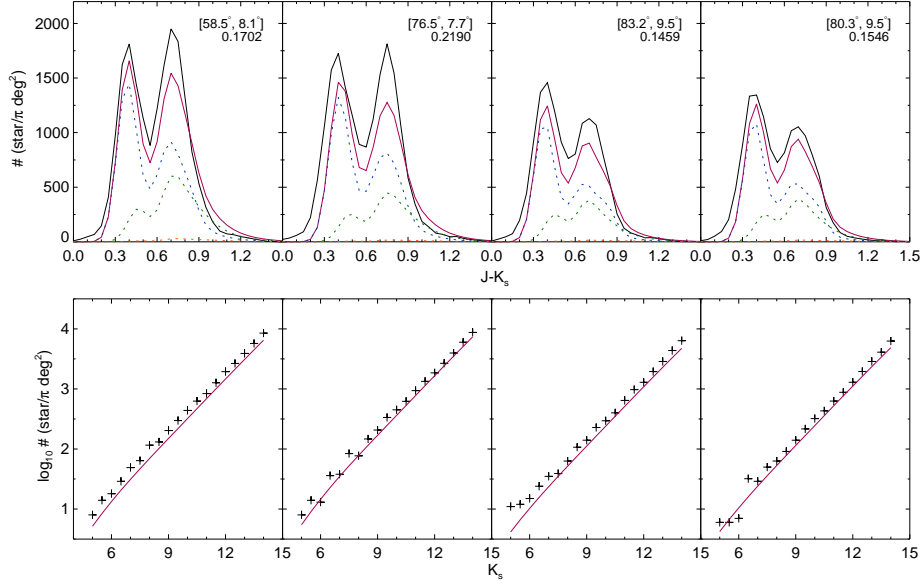


Fig. 9.— The number inconsistency between the model prediction and the 2MASS CD. The upper panel is the comparison of CDs. The upper-right corner shows the coordinates and the extinction $E(J - K_s)$ value. The solid-black, solid-pink, dotted-blue, dotted-green and dotted-orange represent the 2MASS CD, the model prediction, the thin disk, the thick disk and the halo, respectively. The lower panel is the comparison of star counts between 2MASS data (plus) and the model prediction (line).

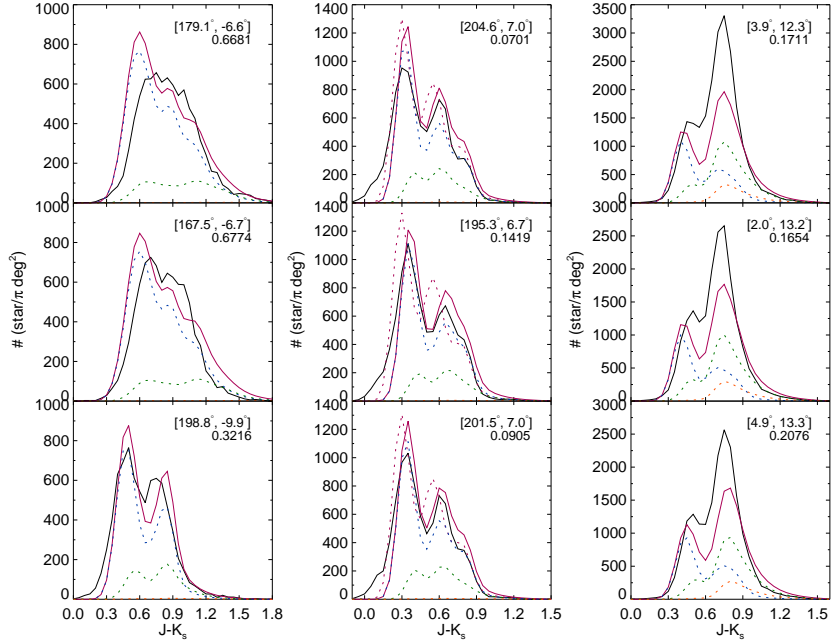


Fig. 10.— The first column shows the improper extinction correction. The second column is the examples of blue population. The third column is the examples in Galactic center region. The solid-black, solid-pink, dotted-pink, dotted-blue, dotted-green and dotted-orange represent the 2MASS CD, the model prediction, the model prediction without extinction correction, the thin disk prediction, the thick disk prediction and the halo prediction, respectively.